2018 IEEE International Conference on Robotics and Automation (ICRA)
May 21-25, 2018, Brisbane, Australia

Optical Fiber-based Sensor for Assessing Electric Current in Unmanned Aerial Vehicles with ROS Interface

Felipe S. Delgado, Marco A. Jucá, André L. M. Marcato and A. Bessa dos Santos

Abstract— **In this work, we propose and experimentally validate a novel optical fiber-based sensor for monitoring and assessing electric current in unmanned aerial vehicles electric motors. The proposed sensing technology combines a Long-Period Fiber Grating sensor and a permanent Neodymium magnet, providing a small and flexible sensing scheme deployed inside the arm of the drone. The experimental results show that good accuracy and linear electric current sensitivity of 0.21 A and 2.08 A/nm, respectively, were achieved with electric current measurements at a 100 Hz sampling rate. The values of hysteresis and repeatability achieved were 0.08 A and 0.22 A, respectively. Finally, a Robot Operating System package for interfacing with the sensing system was developed and tested, which greatly simplifies the deployment of the sensor in robotics applications.**

I. Introduction

Recently, the development and use of unmanned aerial vehicles (UAVs), commonly known as drones, have grown rapidly due to the great importance of this emerging technology for military and civil purposes [1-2], such as aerial mapping, disaster rescue, agricultural irrigation, and military surveillance and attack [3-4].

The UAVs are empowered by different measurement sensors mounted on board. These embedded sensors play an important role in the functioning and performance of the drones, therefore, allowing advanced solutions for a variety of applications [5-8]. Among different types of sensing technologies that could be embedded in drones, the electric current sensors are extremely important since these devices could be used, for example, to monitor and optimize power consumption, provide proper recharging or replacement of the batteries, as well as to determine the health status of the electric motors.

Optical fiber sensors based on Fiber Bragg Gratings (FBGs) and Long-Period Fiber Gratings (LPFGs) are promising real-time techniques for different sensing applications. Over the last few years, the potential of these sensors has been extensively explored in a wide variety of sensing applications [9-11]. In the work reported in [9], Zarrin *et al.* use optical Fiber Bragg Gratings sensors in order to develop a laparoscopic needle driver for measuring axial and grasping force information at the grasper tip with good accuracy and linear sensitivity. Whereas in [10], the FBG sensing technology has been integrated into needle-sized continuum robots in order to provide accurate and sensitive curvature, torsion and force measurements. In addition, Shahriari *et al.*, reported strain measurements from an array of FBG sensors and used the information for online reconstruction of a needle shape in 3D-space [11]. Furthermore, fiber-based sensors have advantageous characteristics, such as robustness, small size, flexibility and immunity to high voltage and external electromagnetic interference [12-13]. Therefore, the deployment of these fiber sensors inside the UAV arm is an appropriate solution for monitoring electric current flowing through a conductor wire of the electrical motor of these aircrafts.

In this work, a novel optical fiber-based sensing system for monitoring and assessing the electric current consumed by a single electric motor of the drone is proposed and experimentally validated. The proposed system, which is composed by a Long-Period Fiber Grating and a permanent Neodymium magnet ($Nd_2Fe_{14}B$), is lightweight, compact and simple to install and thus, could be used near the current conductor wire inside the arm of the UAV. In addition, the mechanism developed to address the electric current consumed by the motor of the aircraft is based on the Lorentz magnetic force. Thus, it is expected that the magnetic field generated by the electrical current flowing within the conductor wire repels the permanent magnet and, therefore, the Neodymium magnet deflection causes strain in the LPFG sensor, which is sensitive to external strain deformation [14-15]. In addition, the use of LPFG-sensors is preferred due to the possibility of further deployments of multi-parameter sensing [16-17] in UAVs applications. Therefore, according to the measurement of the wavelength of the LPFG-sensor data, it is possible to detect the current demanded by the aircraft motor.

Finally, the novel sensing technology is experimentally investigated by fixing the UAV on the laboratory bench and measuring electric current within its entire operating range of 0-10 A and after that, its performance is evaluated by determining the accuracy, hysteresis and repeatability of the proposed sensing scheme.

Additionally, a Robot Operating System (ROS) package was developed to perform the interface between the final calibrated sensing scheme and the embedded computer of the aircraft, which is already using ROS for control purposes. The package simplifies the deployment of the sensor and allows the use of the measured current values within the ROS environment in real time.

This work was supported by Duke Energy, INERGE, ANEEL (Agência Nacional de Energia Elétrica), CAPES, CNPq, FAPEMIG; and by infrastructure grants from the Federal University of Juiz de Fora (UFJF, Brazil).

Felipe S. Delgado, Marco A. Jucá, André L. M. Marcato and A. Bessa dos Santos are with the Electrical Circuit Department, Federal University of Juiz de Fora, Juiz de Fora, Minas Gerais, Brazil (phone: 55 32 9 8805 3331; emails: felipe.souza@engenharia.ufjf.br, marco.juca@engenharia.ufjf.br, andre.marcato@ufjf.edu.br and alexandre.bessa@engenharia.ufjf.br).

Marco A. Jucá is also with the Telecommunications Coordination, Federal Center for Technological Education Celso Suckow da Fonseca, Petrópolis, Rio de Janeiro, Brazil (phone: 55 24 2292 9700).

II. SENSOR DESIGN

A. Long-Period Fiber Gratings

In this study, we focused on a particular type of optical fiber sensor, namely the Long-Period Fiber Grating. LPFGs are optical devices that were firstly introduced by Vengsarkar *et al.* in 1996 [18] for applications in optical communications systems. Since then, the interest in Long-Period Fiber Gratings has rapidly increased, and many papers are available on this topic [19-22].

These in-fiber devices are commonly obtained by generating a periodic modulation of the properties of the optical fiber, normally of the refractive index of the core [23]. Besides, these devices work as wavelength selective optical filters whose wavelength peak (λ) are determined by the period of the LPFG sensor (Λ) and is determined by [18]

$$\lambda = (n_{co} - n_{cl})\Lambda \quad (1)$$

where n_{co} and n_{cl} are the effective refractive index of the core and cladding, respectively.

The LPFG wavelength (λ) shifts due to the sensitivity to mechanical strain deformations, which means that the strain measurement information is inherently encoded in the wavelength. The LPFG wavelength variations due to the strain effect are determined by [24]

$$\frac{\Delta\lambda}{\lambda} = \left[\frac{1}{\Lambda}\frac{\Delta\Lambda}{\Delta\varepsilon} + \frac{1}{n_{co}-n_{cl}}\frac{\Delta(n_{co}-n_{cl})}{\Delta\varepsilon}\right]\Delta\varepsilon \quad (2)$$

where ε is the strain, Λ is the LPFG period, n_{co} and n_{cl} are the effective refractive index of the core and cladding, respectively. Using $\Delta\Lambda/\Lambda = \Delta\varepsilon$ in (1), the wavelength shift can be simplified as [24]

$$\frac{\Delta\lambda}{\lambda} = (1 + p)\Delta\varepsilon \quad (3)$$

where p is the strain-optic coefficient. Therefore, for a specific LPFG sensor, the strain-optic coefficient is known and the wavelength shift is proportional to the strain to which the sensor is subjected.

B. Sensing Principle

The schematic representation of the proposed electric current sensing system is shown in Fig. 1. Dimension constraints control the weight, size and proportions of the designed sensor, therefore, in this work, a permanent Neodymium cubic magnet ($Nd_2Fe_{14}B$), whose dimensions are 6 x 6 x 6 mm, was fixed with epoxy resin in the LPFG sensor, which was fabricated in the Laboratory of Instrumentation and Telemetry (LITel) at the Federal University of Juiz de Fora (UFJF).

The optical device was manufactured in silica core SMF-28 optical fiber with 6 mm length and 125 μm diameter. The designed LPFG is shown in Fig. 2, which is enlarged 10 times.

In addition, a flexible holder was used in order to provide constant support to the optical fiber inserted inside the arm of the aircraft. Therefore, the designed sensor is small and compact and, based upon the requirements of this sensing application, fits very well inside the arm of the aircraft. In order to visualize the reduced size of the proposed sensing head, we can see in Fig. 3 the comparison of its dimension contrasted to a regular sized coin, which has a diameter of 26 mm.

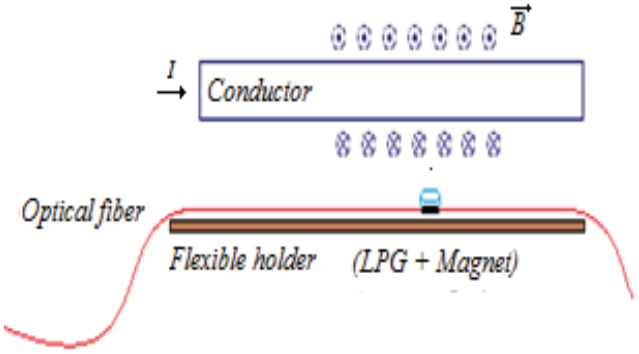

Figure 1. Schematic representation of the proposed optical fiber-based current sensor.

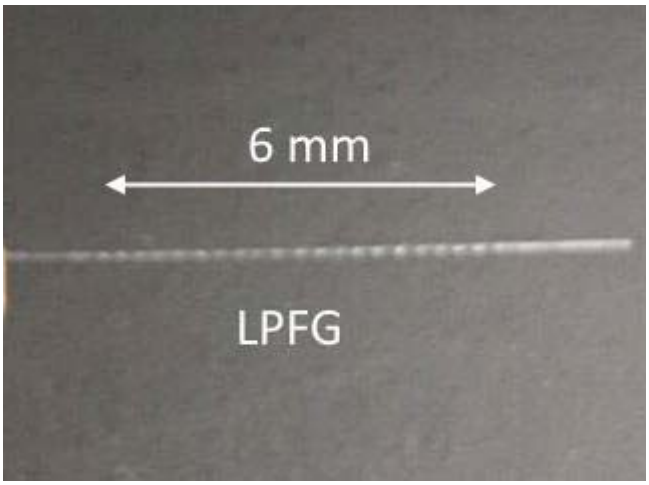

Figure 2. Enlarged view of the designed LPFG sensor.

Another important point to mention is that the distance between the sensing head, which is composed by the LPFG and the permanent Neodymium magnet, was approximately 1 cm and the temperature increase due to the heating of the conductor wire was not significant. For example, the largest temperature variation recorded during the measurements of the electric current through the conductor wire of the UAV motor was 0.1 ºC. Therefore, considering that LPFGs fabricated in standard telecommunications optical fiber normally exhibit temperature sensitivity of approximately 3 nm / 100°C [22,25], the magnitude of the LPFG wavelength shift due to the heating of the conductor wire is insignificant.

Furthermore, it is known that the control signals of the aerial vehicle are transmitted in 2.4 GHz radiofrequency and there are also more communications technologies embedded in the UAV system. For instance, the global positioning system (GPS), onboard as well as telemetry signals. Therefore, these devices generate an electromagnetic interference (EMI) in the surroundings of the aircraft. However, in all realized experimental tests neither this electromagnetic interference had an effect in the permanent magnet displacement nor was significant in the response of

the proposed fiber-based sensing system. It is important to note that this behavior is normal and expected, because the magnet is positioned inside the arm of the aircraft and relatively far from EMI generated by some electronic modules and systems of the UAV, and also due to the well-known immunity of the optical fiber sensors against electromagnetic radiations [26].

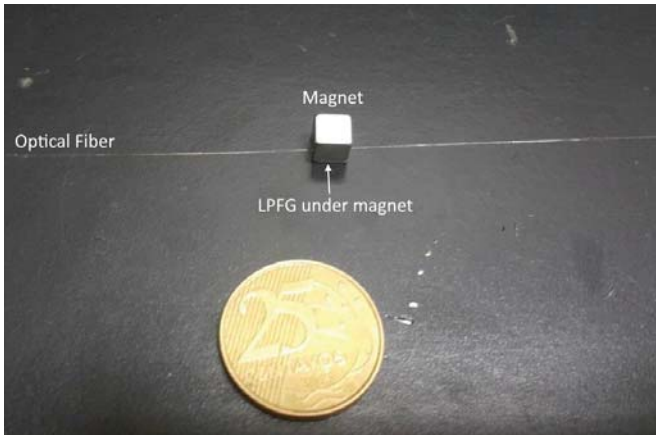

Figure 3. Dimension comparison between the proposed sensing head and a regular sized coin with diameter of 26 mm..

The Neodymium magnet present in the LPFG sensing region can be attracted or repelled depending upon the position of its magnetic poles. In the experiment, we have placed the magnet with the LPFG in order to provide a repulsive electromagnetic force, due to the electrical current I passing through the conductor wire of the UAV motor. The force repels the permanent magnet and thus, causes strain deformation in the LPFG sensor and modifies its wavelengths values. The magnitude of the magnetic force is proportional to the electric current I and can be determined by

$$F = AI \tag{4}$$

where A is a specific constant determined by the distance between the electric current conductor wire and the permanent magnet and its characteristics.

III. Experimental Results

A. LPFG Data Acquisition

In order to measure the wavelength of the LPFG and thus, acquire the sensor data, we have used a commercial optical interrogator FS2200 from FiberSensing. The LPFG interrogator communicates with a personal computer based on local-area network and provides data for the user in high sampling speed for real-time monitoring applications.

Therefore, the sensing system is connected to the optical interrogator and this one is connected to a laptop via the network communication port and UDP protocol. Then, we used a MATLAB program to process the LPFG data and display the electric current measurement to the user. The experimental setup is observed in Fig. 4.

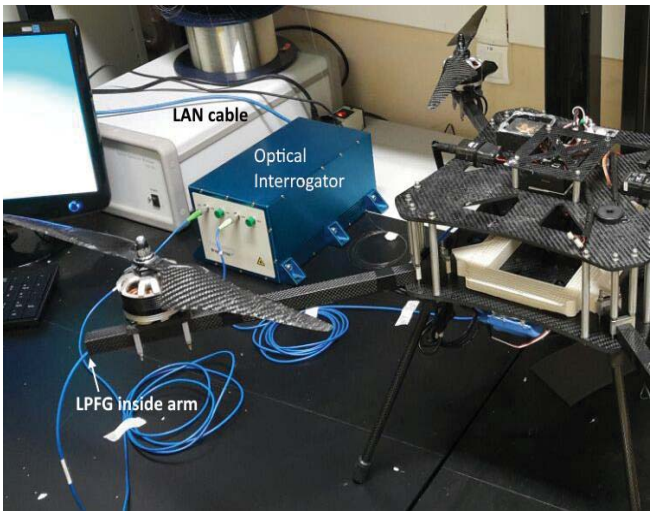

Figure 4. Experimental validation using the proposed sensing system inside the arm of the UAV.

B. Sensor Calibration and Performance

In order to calibrate the electric current sensing system and thus, obtain a relationship between the electric current demanded by the electric motor of the UAV and the measured wavelength of the LPFG, we activated the drone by applying PWM duty cycles ranging from 45-80 %. Therefore, using a digital ammeter clamp (Agilent, U1213A) it is possible to measure the electric current and calibrate the sensor.

The response of the current sensor was experimentally investigated by activating the electric motors of the UAV, however, the measurements were done for only one motor until it reached its maximum value of 10 A. The detailed correlation between the duty cycles of the PWM signals and the electric current drained by a single motor is represented in Fig. 5.

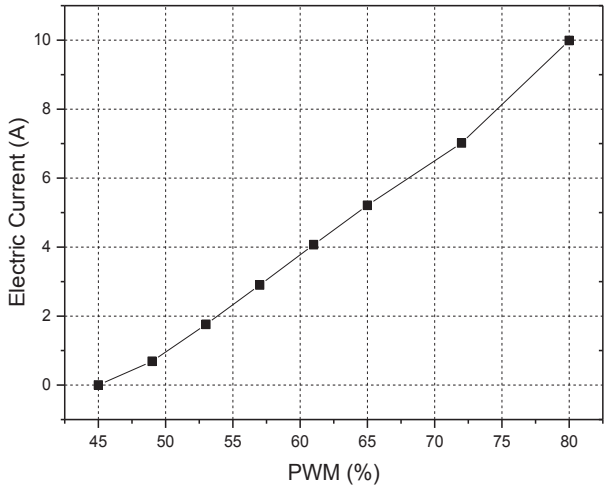

Figure 5. Relation between the values of PWM duty cycle and the electric current consumed by one motor.

During the calibration procedure the LPFG data was acquired and used to perform a linear regression and therefore, establishing a correlation between the response of the LPFG and the digital ammeter. By data fitting using MATLAB, an electric current sensitivity of 2.08 A/nm was achieved with high degree of linearity, which is confirmed by the coefficient of determination $R^2 = 0.999$ derived from the fitting process, as represented in Fig. 6. In addition, the error bars in Fig. 6 represent the wavelength measurement error due to the intrinsic properties of the LPFG sensor and the optical interrogator. Furthermore, we expect that this wavelength uncertainty observed during the experimental tests may influence in the performance metrics, such as accuracy and repeatability, of the model obtained from the linear regression to represent the proposed electric current sensing system, however, these metrics would be acceptable for the current domain ranging from 0-10 A of the sensing application.

Thereafter, we repeated the same experimental process five times, with the electric motor of the UAV draining electric current ranging from 0-10 A, in order to analyze the performance of the current sensor. This way, the hysteresis, the accuracy and the repeatability of the sensing system were determined.

Firstly, the hysteresis of the sensing system was determined by comparing the root-mean-square error (RMSE) during acceleration and deceleration of the drone, as shown in Fig. 7. Then, accuracy was estimated by comparing the RMSE between the measured electric current values by the sensing system and the digital ammeter clamp. After that, the repeatability of the sensor was obtained by determining the standard deviation of the error in each experimental test performed. The performance results of the electric current sensor were determined in electric current unit (A) and can be observed in Table I. We can note that the proposed sensing scheme follows the commercial digital ammeter clamp accurately with good repeatability and low hysteresis within the electric current domain varying from 0 A to 10 A. As far as we are concerned, these good metrics are associated with the mechanical design of the proposed sensing scheme, as well as the use of a high quality lab bench optical interrogator.

Furthermore, the performance results could be further improved by modifying the mechanical structure of the sensing scheme. For example, alternative methods of embedding the LPFG fiber and the magnet in the flexible holder could be contemplated. In the current design, we glued the permanent magnet and the LPFG sensor with epoxy resin and, therefore, it would be interesting to investigate possible long-term effects that may lead to erroneous measurement of electric current and change it if necessary.

Another important issue is that the lab bench optical interrogator is inappropriate for the real on-board application. Thus, the real on-board sensing scheme, which consists mainly of a LED source, the LPFG attached to the permanent magnet and photodetectors, instead of the commercial optical interrogator, has the advantage of small size and being compact. Therefore, the real size of the on-board hardware would be smaller than the size of some embedded modules in the aircraft, for instance, telemetry modules, electronic speed controller, FPV camera and transmitter and power distribution board. In addition, we expect that by changing the interrogation hardware from the commercial one to a real on-board hardware, a variation of the electric current sensitivity and performance results, such as hysteresis, accuracy and repeatability. However, these metrics might remain acceptable as long as an adequate design of the on-board optical interrogator is performed.

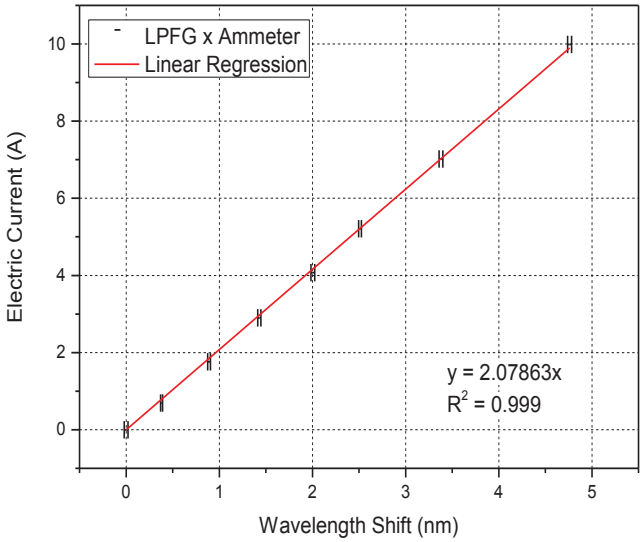

Figure 6. Calibration curve of the LPFG sensor using a digital ammeter clamp.

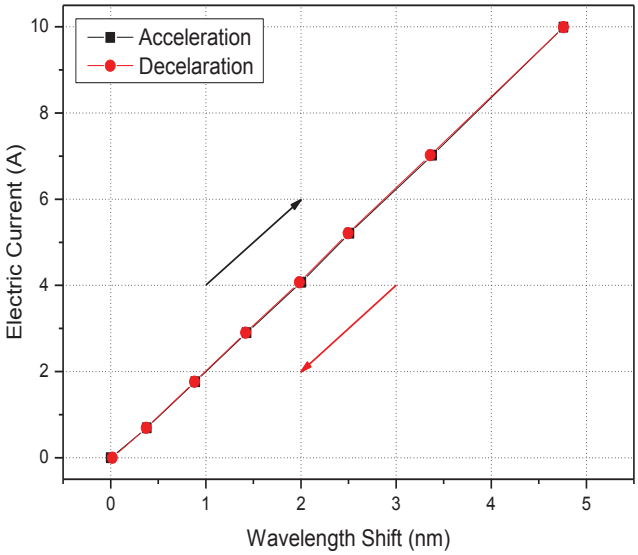

Figure 7. Hysteresis curve for electrical current measurent with the LPFG sensor.

TABLE I. PERFORMANCE VALUES OF THE ELETRIC CURRENT SENSOR.

Hysteresis (A)	*Accuracy (A)*	*Repeatability (A)*
0.0823	0.2052	0.2197

IV. ROS PACKAGE

The UAV built in LITel has an onboard computer running the control algorithms within the ROS environment. Therefore, a ROS package for interfacing with the sensor was developed consisting of an interrogation node and a processing node. The schematic representation of the information flow related to the developed ROS package is depicted in Fig. 8.

The interrogation node is responsible for querying the sensor at a specified sampling rate and publishing the value of the LPFG resonant wavelength into a ROS topic. The sampling rate of the system was chosen as 100 Hz, which is sufficiently high to capture the normal current variation in the motor. The processing node subscribes to the wavelength topic and uses its value, along with the calibration curve obtained, to calculate the electric current corresponding to the measured LPFG wavelength. Finally, this node publishes the current value in amperes into another ROS topic, making it available to any node running in the same ROS environment

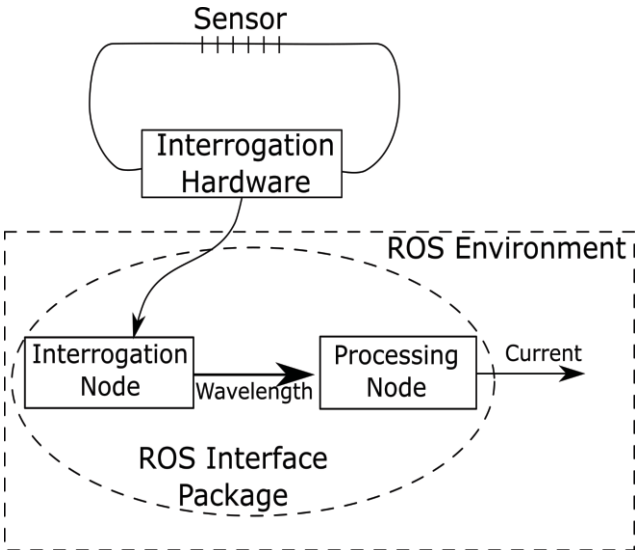

Figure 8. Schematic of the developed ROS package.

.

Another related point to consider about the ROS package is its advantage of being promptly adapted to the new hardware. Therefore, by creating the package, which consists of the interrogation and processing nodes, which can be observed in Fig. 8, the process of adapting it to the onboard interrogation unit would be simplified, since the required modifications in each node are independent of the other node. For that reason, if we change the interrogation hardware, only the interrogation node needs modifications. Conversely, the same package could be used to easily interrogate a number of different types of sensors on a single fiber, such as temperature or strain sensors, by changing only the processing node.

In order to test the package, the whole range of electric current of the motor was interrogated. The current was varied from 0 to 10 A, then back to 0 A linearly during 60 seconds, corresponding to the acceleration and deceleration of the motor, and the results are shown in Fig. 9. The black curve is the current value published by the processing node at 100 Hz. Measurements made with the ammeter clamp are also provided for comparison.

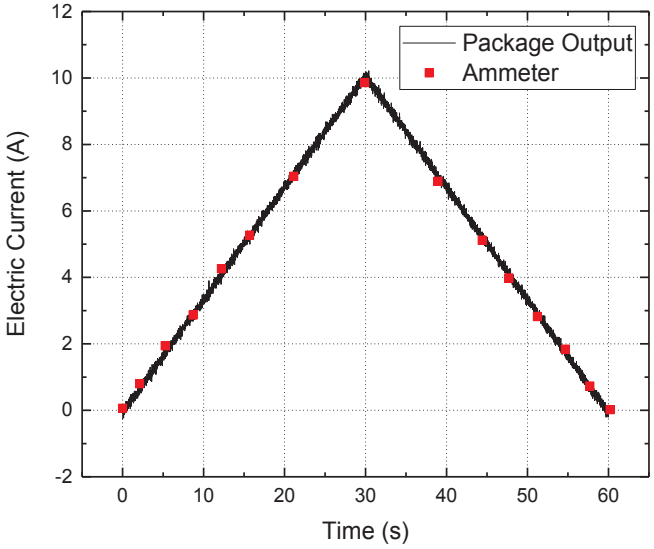

Figure 9. Sensor output processed by the ROS package compared to ammeter clamp.

V. CONCLUSION

A novel optical fiber-based electric current sensor has been proposed and experimentally validated. The novel sensor based upon a Long-Period Fiber Grating sensor combined with a permanent Neodymium magnet as a transducer allows accurate and repeatable measurements of the electric current through the conductor wire of the UAV motor, with low hysteresis. Furthermore, the authors have recently filed a pending patent regarding the proposed sensing technique.

In addition, the introduction of the optical fiber-based sensing system allows the implementation of different optical sensors, which are easily multiplexed, and therefore reducing the overall cost of the sensing system. For example, additional sensors could be used to measure temperature, environmental gases and structural health monitoring (SHM) in the same optical fiber. Therefore, this is an important step towards a highly sensorized aircraft.

It is important to mention that in spite of performing the experimental validation of the current sensing scheme with the UAV fixed on a lab bench, a portable version of the current sensor would be embedded in the drone. This sensing scheme would consist of an LED light source, the LPFG and the permanent Neodymium magnet, photodetectors and a simple electronic unit and, therefore, allowing its application in real conditions.

The developed ROS package allows the end user to easily incorporate the sensing scheme to a working ROS environment, providing real-time current measurements that can be used by other ROS nodes. Importantly, the package can work with the portable interrogation hardware with little change to the interrogation node.

ACKNOWLEDGMENT

The authors would like to thank Italo Fernando Valle Alvarenga for his help with the LPFG sensor fabrication and João Pedro Carvalho de Souza for his collaboration with the development and mechanical design of the UAV. Thanks are also specially due to Prof. Daniel Discini Silveira for his suggestions and contributions to this work.

REFERENCES

[1] S. Zingg, D. Scaramuzza, S. Weiss and R. Siegwart, "MAV navigation through indoor corridors using optical flow," 2010 IEEE International Conference on Robotics and Automation, Anchorage, AK, 2010, pp. 3361-3368.

[2] R. Schacht-Rodriguez, G. Ortiz-Torres, C. D. García-Beltrán, C. M. Astorga-Zaragoza, J. C. Ponsart and D. Theilliol, "SoC estimation using an Extended Kalman filter for UAV applications," 2017 International Conference on Unmanned Aircraft Systems (ICUAS), Miami, FL, USA, 2017, pp. 179-187.

[3] J. Wang, C. Jiang, Z. Han, Y. Ren, R. G. Maunder and L. Hanzo, "Taking Drones to the Next Level: Cooperative Distributed Unmanned-Aerial-Vehicular Networks for Small and Mini Drones," in IEEE Vehicular Technology Magazine, vol. 12, no. 3, pp. 73-82, Sept. 2017.

[4] L. Gupta, R. Jain, and G. Vaszkun, "Survey of important issues in UAV communication networks," Commun. Surveys Tuts., vol. 18, no. 2, pp. 1123–1152, 2015.

[5] L. Moraes et al., "Autonomous Quadrotor for accurate positioning," in IEEE Aerospace and Electronic Systems Magazine, vol. 32, no. 3, pp. 58-62, March 2017.

[6] N. Gageik, M. Strohmeier, S. Montenegro, "An autonomous UAV with an optical flow sensor for positioning and navigation", International Journal of Advanced Robotics, vol. 10, 2013.

[7] M. Itkin, M. Kim, and Y. Park, "Development of Cloud-Based UAV Monitoring and Management System," Sensors, vol. 16, no. 11, p. 1913, Nov. 2016.

[8] T. Villa, F. Salimi, K. Morton, L. Morawska, and F. Gonzalez, "Development and Validation of a UAV Based System for Air Pollution Measurements," Sensors, vol. 16, no. 12, p. 2202, Dec. 2016.

[9] P. S. Zarrin, A. Escoto, R. Xu, R. V. Patel, M. D. Naish and A. L. Trejos, "Development of an optical fiber-based sensor for grasping and axial force sensing," 2017 IEEE International Conference on Robotics and Automation (ICRA), Singapore, 2017, pp. 939-944.

[10] R. Xu, A. Yurkewich and R. V. Patel, "Curvature, Torsion, and Force Sensing in Continuum Robots Using Helically Wrapped FBG Sensors," in IEEE Robotics and Automation Letters, vol. 1, no. 2, pp. 1052-1059, July 2016.

[11] N. Shahriari, R. J. Roesthuis, N. J. van de Berg, J. J. van den Dobbelsteen and S. Misra, "Steering an actuated-tip needle in biological tissue: Fusing FBG-sensor data and ultrasound images," 2016 IEEE International Conference on Robotics and Automation (ICRA), Stockholm, 2016, pp. 4443-4449.

[12] J. L. Santos et al., "Optical fibre sensing networks," 2009 SBMO/IEEE MTT-S International Microwave and Optoelectronics Conference (IMOC), Belem, 2009, pp. 290-298.

[13] J. M. Lopez-Higuera, Handbook of Optical Fibre Sensing Technology; Wiley: New York, NY, USA, 2002.

[14] K.-P. Ma, C.-W. Wu, T.-S. Hsieh, M.-Y. Hsieh, and C.-C. Chiang, "Application of Robust, Packaged Long-Period Fiber Grating for Strain Measurement," Micromachines, vol. 7, no. 8, p. 129, Jul. 2016.

[15] W. Yi-Ping, X. Limin, D. N. Wang and W. Jin, "Highly sensitive long-period fiber-grating strain sensor with low temperature sensitivity," Opt. Lett. 31, 3414-3416, 2006.

[16] F. S. Delgado and A. Bessa dos Santos, "Multi-measurement scheme for a fiber-optic sensor based on a single long-period grating," Journal of Modern Optics, vol. 64, no. 21, pp. 2428-2432, 2017.

[17] F. S. Delgado, D. D. Silveira, T. V. N. Coelho and A. Bessa dos Santos, "Mathematical modelling for correlation between temperature and mechanical strain in long period gratings," IEEE SENSORS 2014 Proceedings, Valencia, 2014, pp. 1900-1903.

[18] A. M. Vengsarkar, P. J. Lemaire, J. B. Judkins, V. Bhatia, T. Erdogan and J. E. Sipe, "Long-period fiber gratings as band-rejection filters," in Journal of Lightwave Technology, vol. 14, no. 1, pp. 58-65, Jan 1996.

[19] F. Esposito, R. Ranjan, S. Campopiano and A. Iadicicco, "Experimental Study of the Refractive Index Sensitivity in Arc-induced Long Period Gratings," in IEEE Photonics Journal, vol. 9, no. 1, pp. 1-10, Feb. 2017.

[20] S. A. Vasiliev and O. I. Medvedkov, "Long-period refractive index fiber gratings: Properties, applications, and fabrication techniques," Proc. SPIE, vol. 4083, pp. 212–223, 2000.

[21] A. Iadicicco, D. Paladino, P. Pilla, S. Campopiano, A. Cutolo, and A. Cusano, "Long period gratings in new generation optical fibers," in Recent Progress in Optical Fiber Research, Rijeka, Croatia: InTech., 2012.

[22] S. W. James and R. P. Tatam, "Optical fibre long-period grating sensors: characteristics and application," Meas. Sci. Technol., 14(2003), pp. R49-R61.

[23] A. Vengsarkar, N. Bergano, C. Davidson, J. Pedrazzani, J. Judkins, and P. Lemaire, "Long-period fiber-grating-based gain equalizers," Opt. Lett. 21, 336-338 (1996).

[24] L. Qin, Z.X. Wei, Q.Y. Wang, H.P. Li, W. Zheng, Y.S. Zhang, D.S. Gao, "Compact temperature-compensating package for long-period fiber gratings, " In Optical Materials, Volume 14, Issue 3, 2000, Pages 239-242.

[25] A. Singh, D. Engles, A. Sharma, M. Singh, Temperature sensitivity of long period fiber grating in SMF-28 fiber, Optik - International Journal for Light and Electron Optics, Volume 125, Issue 1, Pages 457-460, 2014.

[26] S. J. Mihailov, "Fiber Bragg Grating Sensors for Harsh Environments," Sensors, vol. 12, no. 2, p. 1898, Feb. 2012.